THE CONSTRUCTON FEATURES OF CRYSTAL LATTICES OF LOW-SYMMETRICAL SUPERSTRUCTURES

Baranov M.A. and Dubov E.A. *e-mail: fap@agtu.secna.ru*
The Altay state technical university, 656038, Barnaul, Russia,

Abstract. The stable state of a low symmetrical crystal lattice of the ordered alloy is reached as a result of minor distortions of its elementary cells stipulated by displacements of atoms relatively knots of geometrically perfect lattice. A random distribution of static displacements of atoms on a volume of a crystal and their independence from a previous history of a sample (its thermo-mechanical treatment, operation conditions of appropriate details) are a reason that the static displacements of atoms appear as the important factor of hardening of low-symmetrical crystals. The quantitative description of static distortions of elementary cells is executed for alloys $AlTi_3$ with a superstructure $D0_{19}$ and $TiNi_3$ with a superstructure $D0_{24}$ on the basis of a hexagonal lattice of knots. On an example of simulation of the equilibrium configurations of vacancies in alloys with superstructures $D0_{19}$ and $D0_{24}$ is shown, that the ignoring of superstructural static distortions of a lattice at studying of low-symmetrical crystals can result in error outcomes and even to artifacts.

Introduction

It is conventional to present time [1-3] that higher strength properties of the ordered alloys are explained by presence at them specific types of defects - antiphase boundaries, super partial dislocations, defects of substitution etc. The distortions arising near these defects in comparison with metals and disordered alloys are additional barrier for sliding of dislocations. Said fully take place in alloys of high-symmetrical superstructures - B2, $L1_2$, $L1_0$ etc. i.e. such, in which each atom of a perfect crystal has symmetrical environment by other atoms.

In crystals of low-symmetrical superstructures - $D0_3$, $L2_1$, $D0_{19}$, $D0_{24}$ and many others owing to asymmetric arrangement of atoms on knots of elementary cell the stable state of a crystal lattice is reached in result of its distortion. It is fair to term these distortions as superstructural, because they are characteristic of a crystal of a considered superstructure irrespective of its previous history. The displacements of atoms, stipulated by superstructural distortions, are inappreciable in comparison with interatomic distances. However, being uniformly distributed on all volume of a crystal, they become the important factor of its hardening. The values of static displacements of atoms stipulated by superstructural distortions can be gauged experimentally with the help, for example, diffraction methods [4]. However, owing to a smallness of these displacements, the accuracy of the measurements should be enough high. An alternate research technique of superstructural distortions is the computer simulation. Let's consider application of this method on an example of superstructures $D0_{19}$ and $D0_{24}$.

Stability of crystal lattices of alloys with superstructures $D0_{19}$ and $D0_{24}$.

The stoichiometric formula of superstructures $D0_{19}$ and $D0_{24}$ is AB_3 [5]. Their structure can be presented as stacked in pile of identical layers of the hexagonal configuration. Each of layers is filled by atoms of sorts A and B in a stoichiometric relationship. And the atoms of A sort also form a hexagonal grid with the size of a cell twice exceeding distance between the nearest atoms in a layer. The sequence of stacking of layers in a superstructure $D0_{19}$ is abababab and corresponds to stacking of layers in lattice of HCP metal. In a superstructure $D0_{24}$ the sequence of stacking of layers is abacabacabac and corresponds to stacking of layers in α-Lanthanums lattice. Thus, owing to affinity of crystal-geometrical construction of indicated superstructures the application of the unified approach to their consideration is meaningful.

The elementary cell of that and other superstructure can be chosen as a 120-degree prism located in four neighboring layers. As the sizes of elementary cells of these of superstructures usually accepted a_0 - distance between nearest atoms of A sort in the basic layer and c_0 - width of a crystal falling on four basic layers. Usually instead of c_0 the axial ratio $\eta=c_0/a_0$ is used. That is, in superstructures $D0_{19}$

and $D0_{24}$ there is allocated direction - normal to a basic plane (0001) that testifies about anisotropy of such crystal lattices.

The stable state of hexagonal crystals at the experimentally observable sizes of elementary cells, generally speaking, cannot be described within the framework of model spherically-symmetrical central pair potentials. Apparently, that uncentrality of interatomic interactions is a reason of anisotropy of such crystals and, in turn, is stipulated by unsphericity of electronic shells of atoms.

In [6-7] for the description of interatomic interactions in HCP metals the potential function was offered. It is dependent not only on length r of vector **r** of interatomic bond, but also on its direction.

$$\varphi(\vec{r}) = (1 + \xi \cdot \cos^2\theta) \cdot \varphi_M(r), \tag{1}$$

where θ - is angle between vector of interatomic bond and main axis of a crystal.

$$\varphi_M(r) = D\beta e^{-\alpha r}(\beta e^{-\alpha r} - 2) \tag{2}$$

potential Morse - function traditionally used for simulation of defects in cubic crystals; ξ , α, β, D – parameters. In [9] the potential function (1) was applied to definition of elastic modules of alloys with superstructures $D0_{19}$ and $D0_{24}$. The potentials linking atoms of identical sorts were supposed the same, as in pure metals. The parameters of potentials linking atoms of different sorts were determined from stability conditions of a crystal lattice of alloy at the experimentally observable sizes of elementary cells. These conditions can be recorded as

$$\left.\begin{aligned} U_{all}(a_0,\eta) &= -(n_A E_A + n_B E_B + H_{all}) = -E_{cell} \\ \frac{dU_{all}(a_0,\eta)}{da_0} &= 0 \\ \frac{dU_{all}(a_0,\eta)}{d\eta} &= 0 \end{aligned}\right\} \tag{3}$$

Where E_{cell} - bond energy of alloy in calculation on a cell; E_A and E_B - bond energy of metals A and B; n_A and n_B - numbers of atoms of A and B sort in elementary cell; H_{all}- a heat of an alloyage, which for different alloys on an order of magnitude makes 3-5 % from total bond energy of components; U_{all} (a_0,η) - internal energy of alloy in calculation on the elementary cell, introduced as the total of energies of pair interatomic interactions of a view (1)

$$U_{all} = \frac{1}{2}\sum_i \sum_j \varphi_{(p_i),(q_j)}\left(\vec{r}_i - \vec{r}_j\right) \tag{4}$$

Where i - number of a knot of elementary cell, and j - number of a knot from i-th environment; p_i and q_j - sorts of atoms located in an i-th and in j-th knots. That is, the couple of indexes p_i and q_j determines a sort of an interatomic potential A-A, A-B or B-B. The interactions were taken into account to the sixth coordination sphere that in hexagonal crystals makes 38 interatomic bonds. For comparison: three-spherical potentials in FCC and BCC lattices usually used at simulation of defects are taken into account interactions with 42 and 26 neighbours accordingly.

To supply stability of a lattice of considering superstructure concerning its transition in a disorder state or in a state with other ordered disposition of atoms, the criterion of an acceptability of antiphase boundary formation energy value in basic plane was used. For this purpose available experimental data [8] for some alloys were compared with corresponding obtained data. According to such scheme the parameters of interatomic potentials linking atoms of every possible sorts in some alloys of superstructures $D0_{19}$ and $D0_{24}$ were determined. The values of these parameters, as well as experimental data about the sizes of elementary cells of alloys are resulted in the table 1. The view of interatomic poten-

tials for alloy $TiNi_3$ is adduced in a fig. 1. The most visual performance about behaviour of interatomic potentials linking atoms of every possible sorts can be receive from consideration of their lines of constant values. For alloy $TiNi_3$ they are resulted in a fig.2. As it is visible from a fig. 2 a) for the spherically symmetrical potential Ni-Ni these lines are circles. The minima of potentials Ti-Ti and Ni-Ni are reached in directions parallel the basic plane, that is typical for metals with an axial ratio $\eta<1{,}633$. In metals and alloys with $c_0/a_0 > 1{,}633$ the appropriate minima are reached in directions parallel to axis Z.

Table 1. Initial experimental data and parameters of interatomic potentials (3) for alloys with superstructures $D0_{19}$ and $D0_{24}$

Alloy, super-structure	Initial data, source		Type of the bond	Parameters of the potential			
	a_0, Å	$\eta_{exper.}$		ξ	α, Å^{-1}	β	D, eV
WCo_3, DO_{19}	5.13 [5]	1.61014 [5]	Co-Co	-0.25480	1.41228	45.8561	0.53795
			Co-W	-0.30481	1.77388	115.6713	0.93372
			W-W	0.0	1.40873	62.6848	1.13016
$MoCo_3$, DO_{19}	5.13 [9]	1.60624 [9]	Co-Co	-0.25480	1.41228	45.8561	0.53795
			Co-Mo	-0.36151	1.84795	137.4457	0.84389
			Mo-Mo	0.0	1.45763	69.7440	0.90043
$AlTi_3$, DO_{19}	5.793 [10]	1.60711 [10]	Ti-Ti	-0.46777	1.04914	30.1143	0.58133
			Ti-Al	-0.09798	1.82980	212.2137	0.58968
			Al-Al	0.0	1.02635	27.4642	0.31789
$TiNi_3$, DO_{24}	5.101 [5]	1.62845 [5]	Ni-Ni	0.0	1.36720	41.2911	0.47119
			Ni-Ti	-0.28935	1.02725	21.3633	0.53333
			Ti-Ti	-0.46777	1.04914	30.1143	0.58133
$HfPd_3$, DO_{24}	5.595 [9]	1.64290 [9]	Pd-Pd	0.0	1.54072	86.0102	0.48587
			Pd-Hf	-0.13945	1.28686	48.5459	0.71841
			Hf-Hf	-0.48839	0.97173	30.3060	0.76712
$TiPd_3$, DO_{24}	5.489 [9]	1.63308 [9]	Pd-Pd	0.0	1.54072	86.0102	0.48587
			Pd-Ti	-0.41789	1.25706	40.8011	0.61751
			Ti-Ti	-0.46777	1.04914	30.1143	0.58133
$ZrPd_3$, DO_{24}	5.612 [9]	1.64558 [9]	Pd-Pd	0.0	1.54072	86.0102	0.48587
			Pd-Zr	0.00859	1.31860	54.2784	0.62937
			Zr-Zr	-0.44977	0.83723	21.4452	0.68484
$HfPt_3$, DO_{24}	5.636 [9]	1.63378 [9]	Pt-Pt	0.0	1.57871	97.7855	0.73741
			Pt-Hf	-0.25095	1.26331	47.0464	0.89364
			Hf-Hf	-0.48839	0.97173	30.3060	0.76711
$ZrPt_3$, DO_{24}	5.644 [9]	1.63448 [9]	Pt-Pt	0.0	1.57871	97.7855	0.73741
			Pt-Zr	-0.11256	1.45287	77.2155	0.83368
			Zr-Zr	-0.44977	0.83723	21.4452	0.68484

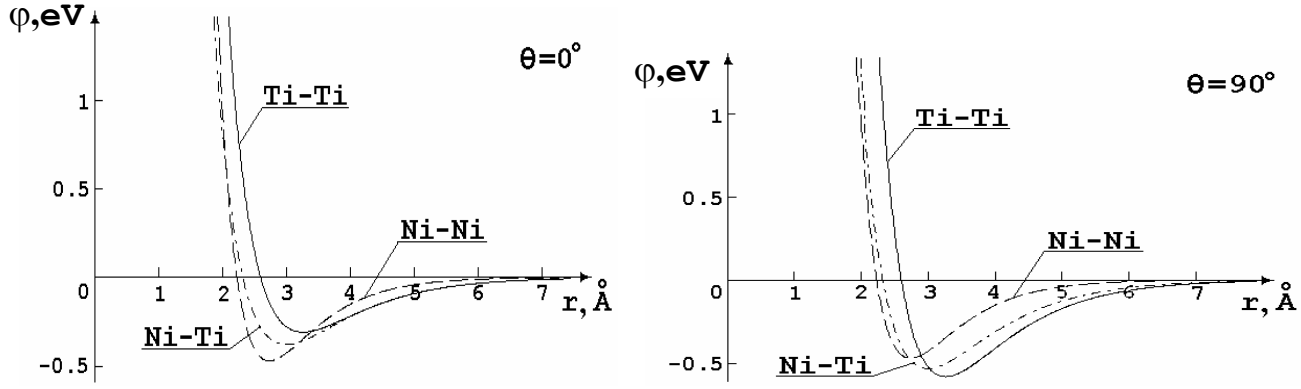

a) b)

Fig. 1 View of interatomic potentials in $TiNi_3$ alloy. a) $\theta=0^0$; b) $\theta=90^0$.

The constructed interatomic potentials were subjected to the subsequent check. On this purpose a minimum of internal energy (4) on parameters a_0 and η at fixed ξ , α, β, D was found and compared to a bond energy of a cell. The values a_{0min} and η_{0min} at which this minimum was reached were compared with corresponding experimental data. For all alloys from the table 1 deviations of the indicated values from included in a system (3) at construction of potentials were watched not less than in the sixth significant digit.

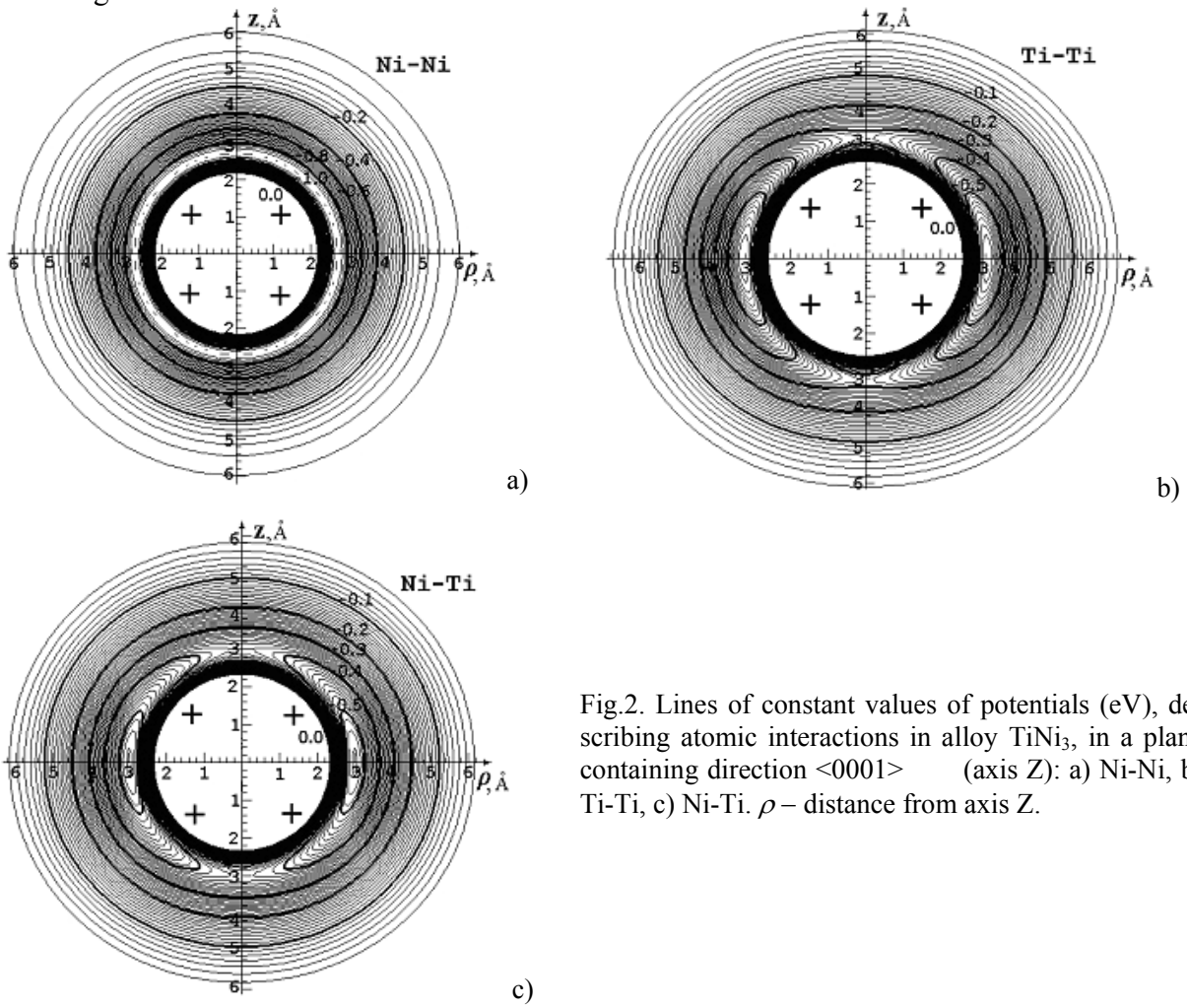

Fig.2. Lines of constant values of potentials (eV), describing atomic interactions in alloy $TiNi_3$, in a plane containing direction <0001> (axis Z): a) Ni-Ni, b) Ti-Ti, c) Ni-Ti. ρ – distance from axis Z.

Superstructural distortions of a lattice

Thus, within the framework of offered model a stable state of a superstructure is reached when nucleus of atoms forming a crystal disposed in knots of an ideal lattice. However, as it was indicated above, more stable state of crystals of low symmetrical of superstructures, what are $D0_{19}$ and $D0_{24}$ is reached as a result of minor distortions of elementary cells. The computer model of the distortion crystal was obtained with the help of so-called method of a superstructural relaxation SSR. The method is based on the assumption that in the ordered crystal without of defects the environment of everyone atom of one and the same sublattice is identical, and average sizes of elementary cells remain the same, as before to a superstructural relaxation. Each sublattice as a unit was submitted a capability to displace in a direction of force acting at it from other sublattices down to achievement of a stablest state. The superstructure $D0_{19}$ was represented consisting from eight sublattices, and $D0_{24}$ - from sixteen ones. The values E_{sr} of an internal energy reduction of alloys was obtained as a result of a SSR in calculation on structural unit AB_3 (4 atoms) are listed in table 2.

The table 2. Energies of a superstructural relaxation E_{sr} and heat of an alloyage H_{all} of some alloys with superstructures $D0_{19}$ and $D0_{24}$, eV/structural unit

Alloy, superstructure	WCo_3 $D0_{19}$	$MoCo_3$ $D0_{19}$	$AlTi_3$ $D0_{19}$	$TiNi_3$ $D0_{24}$	$TiPd_3$ $D0_{24}$	$HfPd_3$ $D0_{24}$	$ZrPd_3$ $D0_{24}$	$HfPd_3$ $D0_{24}$	$ZrPt_3$ $D0_{24}$
E_{sr}	0.0241	0.0123	0.0276	0.0025	0.0015	0.0158	0.0464	0.0101	0.0071
H_{all}	-	-	1.042	1.450	-	-	-	-	-

From consideration of the table 2 it is visible, that on an order of magnitude the energy of a superstructural relaxation is inappreciable and makes 0,3 - 3 % from value of a heat of an alloyage. As a matter of fact the energy of a superstructural relaxation represents a part of a heat of an alloyage allocated at lattice distortion. As the distortions of a lattice render direct influence on hardening of a crystal, the value E_{sr} can be treated as energy of hardening. However, if at deformation or thermal hardening there is an increase of an internal energy of a crystal, then in result of superstructural distortions take place reduction of it. Therefore lattice of low symmetrical crystal, generally speaking, can not be perfect, and, therefore, can not be transferred in a perfect state by thermo-mechanical treatment or at operations of details having in its compositions appropriate phases.

The pictures of lattices distortions in alloys $AlTi_3$ and $TiNi_3$ stipulated by a superstructural relaxation are resulted in a fig.3-4. Projections of atomic displacement vectors here are resulted. In view of their smallness these vectors were increased in an integer of times (scale of atomic displacements).

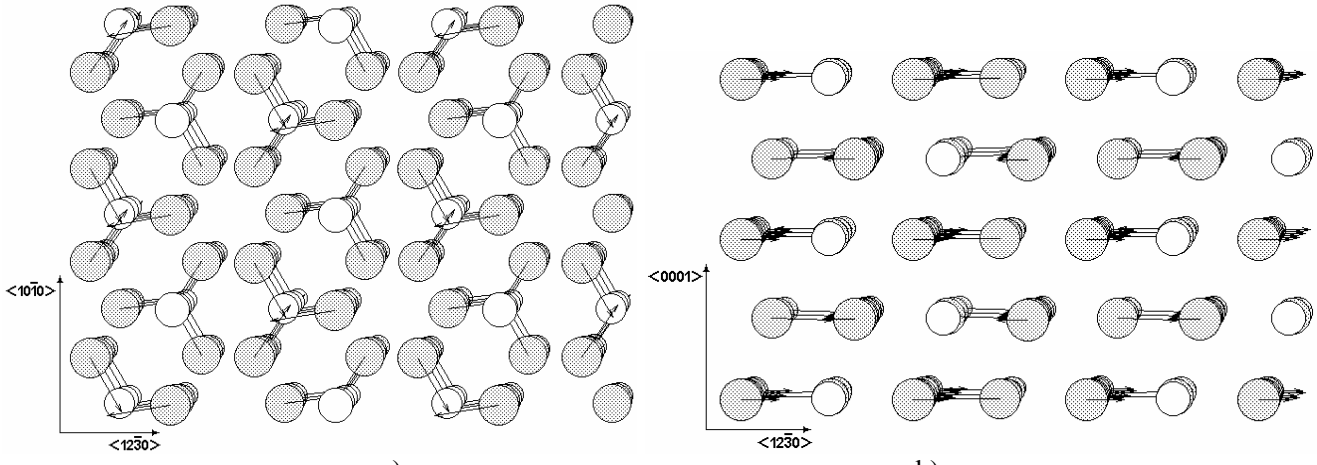

a) b)

Fig. 3. Projection of a crystal lattice of alloy $AlTi_3$ with a superstructure $D0_{19}$ on a plane (0001) - a); and plane $(2\bar{1}\bar{1}0)$ - b). ◎ - atom Ti, ○ - atom Al. Scale of atomic displacements 60:1.

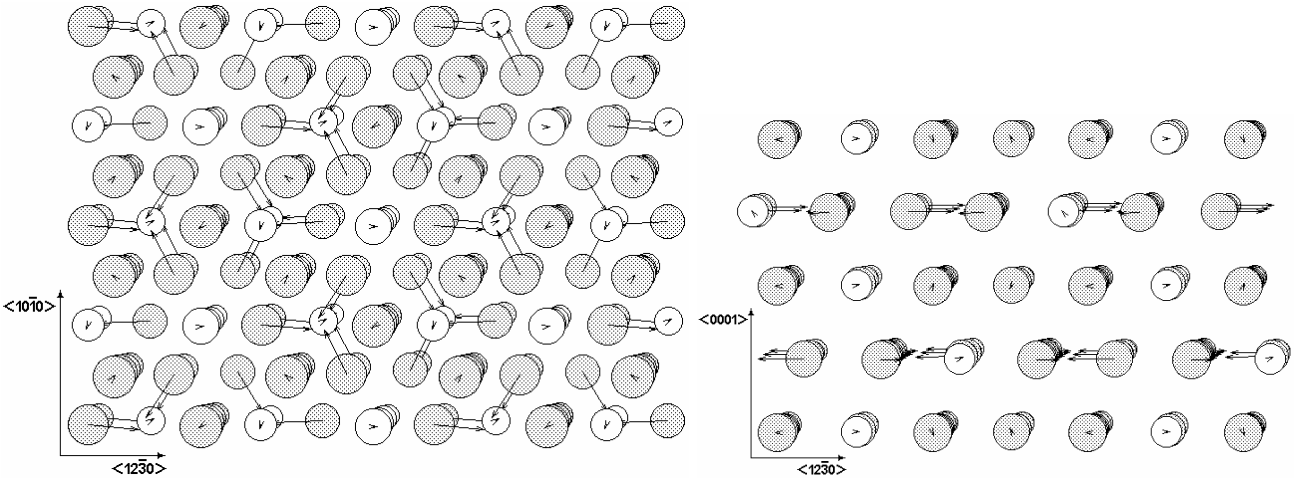

a) b)

Fig. 4. Projection of a crystal lattice of alloy $TiNi_3$ with a superstructure $D0_{24}$ on a plane (0001) - a) and plane $(2\bar{1}\bar{1}0)$ - b). ⊛ - atom Ni, ○ - atom Ti. Scale of atomic displacements 60:1.

From comparison of data of table 2 and pictures of lattice distortions it is possible to make a conclusion about existence of a correlation between size of atomic displacements and the value of SSR energy E_{sr}. At increasing of E_{sr} the amplitude of displacements is increased also. The vectors of atomic displacements are located mainly in a basic plane under angle 60^o to each other.

Simulation of vacancies

The influence of superstructural distortions of low-symmetrical crystals is necessary for taking into account at studying the majority of their physical-mechanical properties. In particular, at construction of the equilibrium configurations of defects it is necessary previously to carry out search of a stablest state of a crystal lattice with the help, for example, superstructural relaxation. If it to not make, it is possible to come to error conclusions and, moreover - to artifacts. Really, at fulfilment of search of the equilibrium configuration of a defect there is a downturn of an internal energy of the computational unit owing to a relaxation stipulated not only by presence of a defect, but also as a result of superstructural distortions. Let's explain said on an example of vacancies.

The simulation of single vacancies, both in metals, and in alloys, was carried out in according with to one and the same procedure. For this purpose in a computer memory the image of the spherical bloc of a crystal of metal or alloy with a given superstructure was formed. The bloc, in turn, was represented consisting from two concentric areas. Radius of internal area relied slightly exceeding the tripled value r_A - radius of action of a potential. External radius was selected equal 5 r_A. The external area placed in space between spheres. The starting configuration of vacancy was formed by deleting atom out of center of the bloc and transferring it on a surface of a crystal. Thus equally half of torn off bonds was restored. As result the starting value of vacancy formation energy E^f_{vs} appeared equal to energy of a sublimation of atom of the given sort from considered sublattice. The vacancies, both in the mentioned above alloys and in pure metals - components of alloys were considered. In metals all knots of a lattice are equivalent for arrangement of vacancy. In the ordered alloys there are some essential distinguishing positions of knotes. In particular, for a superstructure $D0_{19}$ these positions are determined only by sort of deleted atom, and for $D0_{24}$ both sort of atom, and sort of a layer (a or b), in which the vacancy disposed. The layers b and c are equivalent for arrangement of vacancy. The simulation of vacancies was carried out both with preliminary fulfillment of a SSR, and without of it. The obtained values of vacancy formation energies are resulted in the table 3.

Table 3. Values of vacancy formation energies in alloys with $D0_{19}$ and $D0_{24}$ superstructures and in metals - components of researched alloys.

Metal, alloy, type of a lattice	Position of vacancy (sort of atom, layer)	Formation energy, eV			
		Start	Equilibrium, with SSR	Equilibrium, without of SSR	Experiment
1	2	3	4	5	6
Al, A1	—	3.340	—	3.126	0.70
Ni, A1	—	4.434	—	4.210	1.80
Pd, A1	—	3.936	—	3.828	—
Pt, A1	—	5.852	—	5.706	1.51
Mo, A2	—	6.331	—	5.916	3.00
W, A2	—	8.660	—	7.564	3.60
Co, A3	—	5.598	—	4.262	1.91
Hf, A3	—	6.176	—	6.112	—
Ti, A3	—	4.856	—	4.678	—
Zr, A3	—	6.316	—	6.052	—
$AlTi_3$, DO_{19}	Al	4.362	4.349	1.314	—
	Ti	4.822	4.810	1.464	—
$MoCo_3$, DO_{19}	Mo	6.682	6.625	4.200	—
	Co	4.765	4.736	2.534	—
WCo_3, DO_{19}	W	7.986	7.921	4.178	—
	Co	4.982	4.960	1.500	—
$HfPd_3$ DO_{24}	Hf, a	6.795	6.692	3.470	—
	Hf, b	6.850	6.709	3.869	—
	Pd, a	4.357	4.269	1.228	—
	Pd, b	4.500	4.406	1.459	—
$HfPt_3$ DO_{24}	Hf, a	7.741	7.571	4.431	—
	Hf, b	7.863	7.645	4.608	—
	Pt, a	6.024	5.855	2.798	—
	Pt, b	6.195	6.014	3.056	—
$TiNi_3$, DO_{24}	Ti, a	5.411	5.049	1.345	—
	Ti, b	5.668	5.237	1.689	—
	Ni, a	4.400	4.053	0.399	—
	Ni, b	4.628	4.267	0.804	—
$TiPd_3$, DO_{24}	Ti, a	5.204	5.056	3.895	—
	Ti, b	5.288	5.111	3.943	—
	Pd, a	4.096	3.917	2.730	—
	Pd, b	4.203	4.014	2.903	—
$ZrPd_3$, DO_{24}	Zr, a	6.308	6.256	3.348	—
	Zr, b	6.304	6.255	3.780	—
	Pd, a	4.182	4.159	1.412	—
	Pd, b	4.315	4.293	1.592	—
$ZrPt_3$, DO_{24}	Zr, a	7.290	7.201	5.055	—
	Zr, b	7.272	7.157	5.134	—
	Pt, a	5.868	5.794	3.765	—
	Pt, b	5.996	5.922	3.950	—

Experimental values, of vacancy formation energies are known for some metals also here are resulted. The difference between starting values E^f_{vs} obtained with preliminary execution of SSR and without of it is insignificant. Therefore these values are united in third column of the table 3. From the data of the table follows, that in the lattices exposed to the preliminary superstructural relaxation the reduction of vacancy formation energy (column 4) on the second stage of relaxation relatively starting values are small (~1-5% E^f_{vs}). Therefore calculated values of vacancy formation energies are in 2 - 4 times above experimentally observable in metals (column 6), which, in turn, are close to 1эВ. The main reason of such difference, apparently, is that here the single vacancies were considered. In actual samples, on which the experimental researches were carried out, the share of such vacancies is insignificant. The majority of vacancies are adsorbed in places where their energy is low - on extended defects of a lattice - dislocations, grain boundaries, etc. Without the registration of superstructural distortions the relaxational reductions of energy ares great (column 5) and makes 20 - 70% from starting values. However such reduction is stipulated not by vacancy as such, but sizes of the computational unit and superstructural relaxation happening in it.

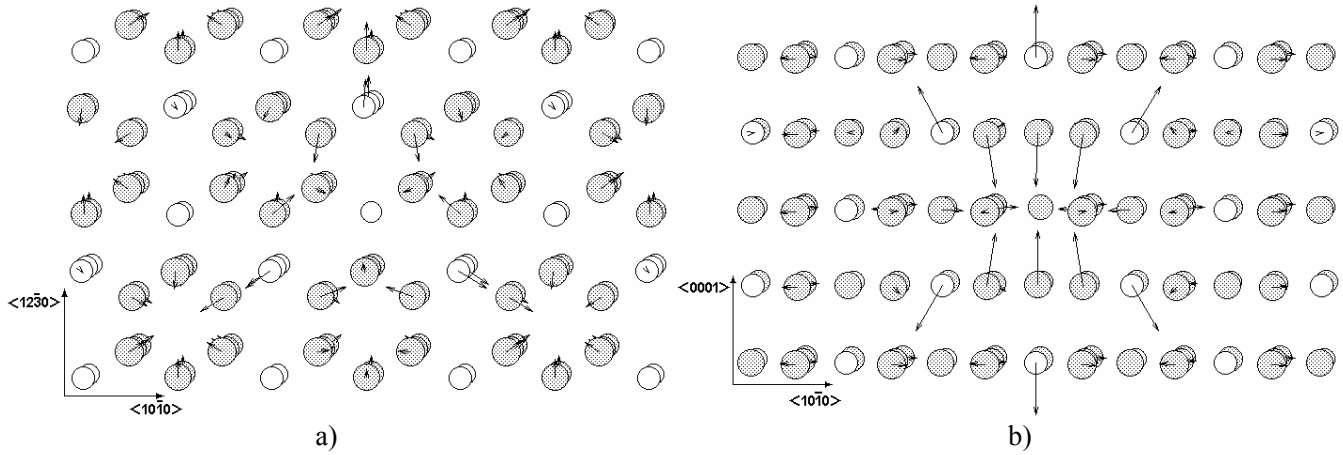

Fig. 5. Equilibrium atomic configuration near the vacancy in $AlTi_3$ alloy, obtained with preliminary superstructural relaxation. Al-deleted atom. Plane of the figure: (0001) – a) and $(01\bar{1}0)$ – b). Scale of the atomic displacements 50:1. ⊛ – Ti atom, ○ – Al atom.

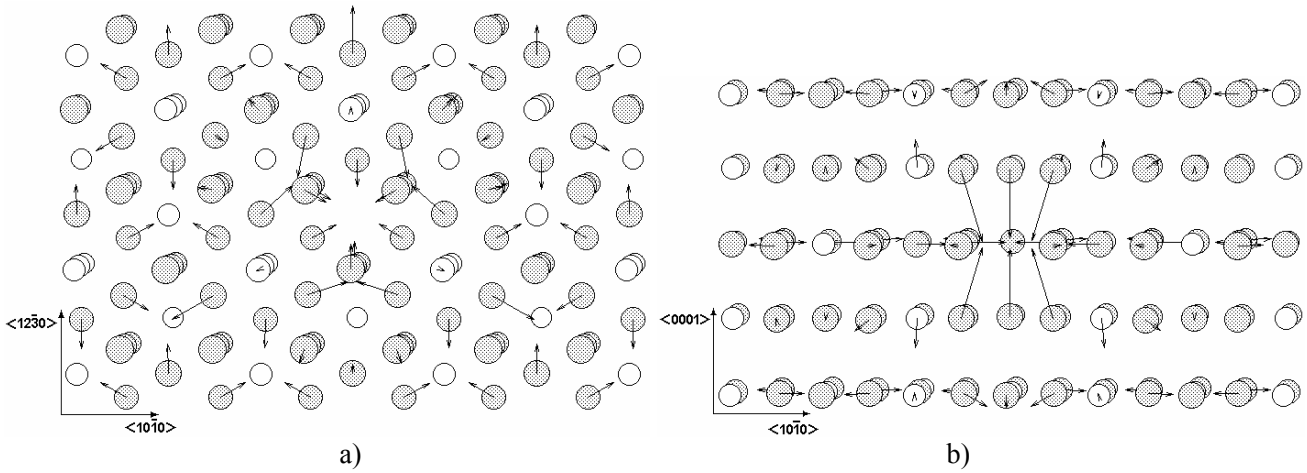

Fig. 6. Equilibrium atomic configuration near the vacancy in $TiNi_3$ alloy, obtained with preliminary superstructural relaxation. Ti-deleted atom from layer b. Plane of the figure: (0001) – a) and $(01\bar{1}0)$ – b). Scale of the atomic displacements 50:1. ⊛ – Ni atom, ○ – Ti atom.

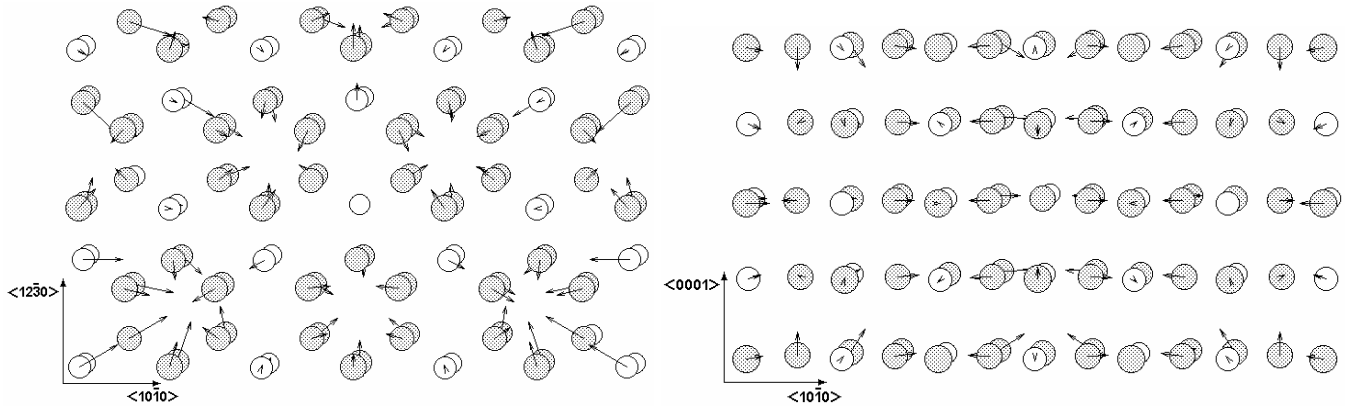

a) b)

Fig. 7. Equilibrium atomic configuration near the vacancy in $AlTi_3$ alloy, obtained without of superstructural relaxation. Al-deleted atom. Plane of the figure: (0001) – a) and $(01\bar{1}0)$ – b). Scale of the atomic displacements 20:1. ⊛ – Ti atom, ◯ – Al atom.

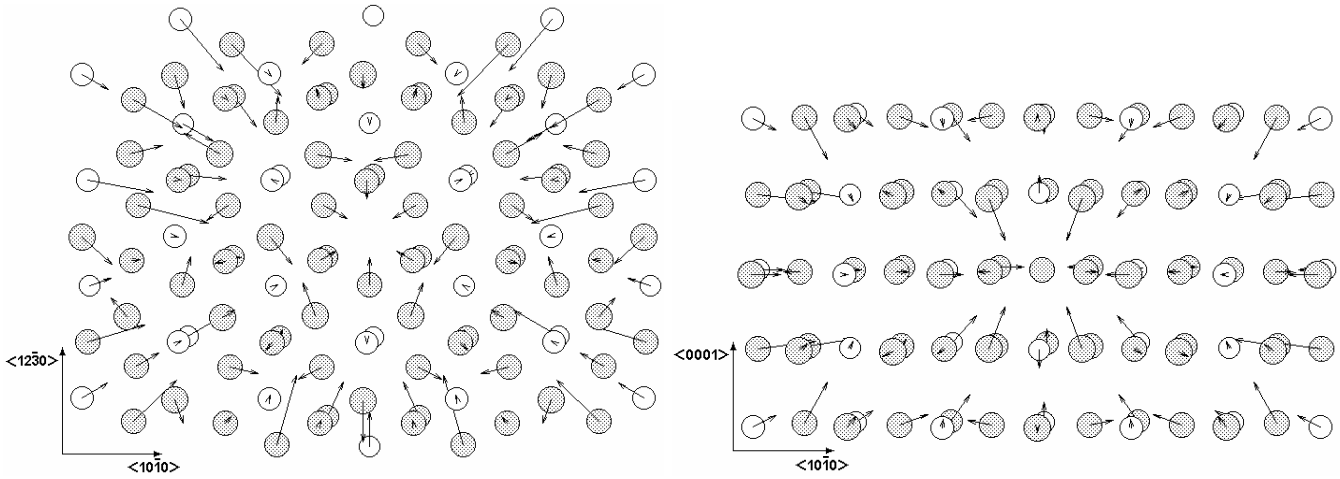

а) б)

Fig. 8. Equilibrium atomic configuration near the vacancy in $TiNi_3$ alloy, obtained without of superstructural relaxation. Ti-deleted atom from layer b. Plane of the figure: (0001) – a) and $(01\bar{1}0)$ – b). Scale of the atomic displacements 20:1. ⊛ – Ni atom, ◯ – Ti atom.

In the figures 5 and 6 the pictures of the atomic configurations arising near vacancies in alloys $AlTi_3$ and $TiNi_3$, obtained with preliminary transfer a crystal in stablest state are resulted. And in the figures 7 and 8 similar pictures for the same alloys obtained for geometrically perfect lattices are resulted. Apparently from figures, that near to single vacancy located in lattice of alloy subjected to the preliminary stabilization with the help of a SSR the atomic displacements approximately twice less, than near to similar vacancy located in a non-stabilized lattice. It is visible from comparison of scale of atomic displacements. The value of atomic displacement in a stabilized lattice decrease at increasing distance between atom and the vacancy. In a non-stabilized lattice it does not occur. It is necessary as a whole the results of vacancy simulation on the basis of a perfect lattice to consider invalid. Thus, the superstructural distortions are one of the important factors providing high strength properties of ordered alloys of low-symmetrical superstructures.

References

1. Kir B.H. Perspective materials. In the world of science. 1986, №12, p. 99-108.(rus).
2. Schtremel M.A. Firmness of alloys. Defects of a lattice. Moscow, Metallurgy, 1982. 280 p. (rus.).
3. Vasilev L.I., Orlov A.N. About mechanisms of hardening of ordered alloys. Physic of metals and metallurgy.1963, v. 15, iss. 3, p. 481-485. (rus.)
4. Selected research techniques in a metallurgy. Edited by H.J. Hunger. Leipzig, 1983. (germ.)
5. Hansen M., Andreco K. Constitution of binary alloys. New-York, Toronto, London. McGraw-hill Book company, 1958, v. 1-2.
6. Baranov M.A., Starostenkov M.D., Romanenko V.V., Dubov E.A., Chernych E.V., Krymskih A.I. State of crystal lattice near stacking faults in HCP metals and alloys. Izvestija VUZov. Physics, 2000, v. 43, p. 38-43. (rus.)
7. Baranov M.A., Dubov E.A., Chernych E.V., Sencova I.V. Elasticity of phases with superstructures $D0_{19}$, $D0_{24}$ allocated at ageing of alloys. Dep. In VINITI 10.10.2003, № 1789-B2003. (rus.).
8. Noskova N.I. Defects and deformation of monocrystals. Ekaterinburg. Dept. of the Russian Academy of science. 1995, 184 p. (rus.)
9. Elliott R.P. Constitution of binary alloys. New-York, St. Louis, San-Francisco, Toronto, London, Sydney. McGraw-hill Book company, 1968, v. 1-2.
10. Shunk F.A. Constitution of binary alloys. New-York, St. Louis, San-Francisco, London, Sydney, Toronto, Mexico, Panama. McGraw-hill Book company, 1971, v.1-2.

Received 10.10.2005